# Functional Morphology of the Pectoral Fins in Bamboo Sharks, *Chiloscyllium plagiosum*: Benthic vs. Pelagic Station-Holding

**Cheryl D. Wilga\* and George V. Lauder**

*Museum of Comparative Zoology, Harvard University, Cambridge, Massachusetts*

ABSTRACT  Bamboo sharks (*Chiloscyllium plagiosum*) are primarily benthic and use their relatively flexible pectoral and pelvic fins to rest on and move about the substrate. We examined the morphology of the pectoral fins and investigated their locomotory function to determine if pectoral fin function during both benthic station-holding and pelagic swimming differs from fin function described previously in leopard sharks, *Triakis semifasciata*. We used three-dimensional kinematics and digital particle image velocimetry (DPIV) to quantify pectoral fin function in five white-spotted bamboo sharks, *C. plagiosum*, during four behaviors: holding station on the substrate, steady horizontal swimming, and rising and sinking during swimming. During benthic station-holding in current flow, bamboo sharks decrease body angle and adjust pectoral fin angle to shed a clockwise fluid vortex. This vortex generates negative lift more than eight times that produced during open water vertical maneuvering and also results in an upstream flow that pushes against the posterior surface of the pectoral fin to oppose drag. In contrast, there is no evidence of significant lift force in the wake of the pectoral fin during steady horizontal swimming. The pectoral fin is held concave downward and at a negative dihedral angle during steady horizontal swimming, promoting maneuverability rather than stability, although this negative dihedral angle is much less than that observed previously in sturgeon and leopard sharks. During sinking, the pectoral fins are held concave upward and shed a clockwise vortex with a negative lift force, while in rising the pectoral fin is held concave downward and sheds a counterclockwise vortex with a positive lift force. Bamboo sharks appear to sacrifice maneuverability for stability when locomoting in the water column and use their relatively flexible fins to generate strong negative lift forces when holding position on the substrate and to enhance stability when swimming in the water column. J. Morphol. 249:195–209, 2001.   © 2001 Wiley-Liss, Inc.

KEY WORDS: bamboo shark; locomotion; station-holding; benthic; pectoral fin; flow visualization; hydrodynamics; *Chiloscyllium plagiosum*

Sharks exhibit a variety of locomotor habits: fast and slow oceanic cruising, generalized continental swimming, slow demersal (epibenthic) locomotion, benthic station-holding, and submerged walking. However, very few species have been studied quantitatively and the limited data available are primarily for epibenthic and pelagic species (Affleck, 1950; Alexander, 1965; Simons, 1970; Thomson, 1976; Videler, 1993; Ferry and Lauder, 1996; Fish and Shannahan, 2000; Wilga and Lauder, 2000). According to the classical model of heterocercal tail locomotion, the head, tail, and pectoral fins of sharks, regardless of locomotor mode, are presumed to generate lift during steady horizontal locomotion (see overview in Lauder, 2000). In contrast, recent research using three-dimensional kinematics in conjunction with fluid dynamic measurement of flow over the pectoral fins indicates that pectoral fins do not generate lift during steady horizontal swimming in two unrelated fishes with heterocercal tails: leopard sharks, *Triakis semifasciata*, and white sturgeon, *Acipenser transmontanus* (Wilga and Lauder, 1999, 2000). The generality of this result is unknown.

Pectoral fins may play a major role during station-holding on the substrate in benthic and pelagic fishes (Webb, 1989; Arnold et al., 1991; Webb et al., 1996; Gerstner, 1998; Gerstner and Webb, 1998). Typical posture for station-holding teleost fishes is standing on the tips of extended pectoral fins while facing upstream (Webb, 1989; Arnold et al., 1991). Dye stream visualization of station-holding salmon parr, *Salmo salar*, indicates that the pectoral fins deflect flow upwards as it passes over the fin surface (Arnold et al., 1991), but no data on the function of pectoral fins in sharks during benthic station-holding are available. Furthermore, the anatomical specializations in the pectoral fins of benthic sharks might alter pectoral fin function during steady swimming and maneuvering in open water.

\*Current address and correspondence to: Dr. Cheryl Wilga, Department of Biological Sciences, University of Rhode Island, 100 Flagg Road, Kingston, RI 02881-0816. E-mail: cwilga@uri.edu

To examine how a benthic lifestyle affects the function of the pectoral fins during locomotion in sharks, we studied both benthic station-holding and pelagic steady horizontal locomotion and vertical maneuvering in a benthic shark, the white-spotted bamboo shark *Chiloscyllium plagiosum* (Hemiscyllidae, Orectolobiformes). We used 3D kinematics and digital particle image velocimetry (DPIV) to quantify the position of the pectoral fins and patterns of fluid flow over the fins. Our goal was to quantify the function of pectoral fins in benthic bamboo sharks in order to 1) clarify the fluid-dynamic mechanisms used during benthic station-holding as well as pelagic station-holding (steady horizontal swimming), 2) quantify the conformation and three-dimensional orientation of the pectoral fins, and 3) compare these data to previous results from sturgeon and leopard sharks that exhibit epibenthic locomotor patterns.

## MATERIALS AND METHODS
### Animals

Five bamboo sharks, *Chiloscyllium plagiosum,* were obtained from the Oregon Coast Aquarium and Seaworld of San Diego. Sharks were housed in 70-l aquaria maintained at a temperature of $25 \pm 2°C$ and fed a diet of smelt. Kinematic and DPIV experiments were performed on these individuals, which ranged from 25–50 cm in total length ($l$) (mean 37 cm). Experiments were conducted in a calibrated flow tank maintained at an average temperature of $25 \pm 0.5°C$ (see Jayne and Lauder, 1995; Drucker and Lauder, 1999; Wilga and Lauder, 1999).

### Morphology

The skeletal and muscular elements of the pectoral fin and adjacent trunk region thought to be involved in locomotion were dissected and described using five fresh-frozen specimens. Sharks (25–50 cm $l$) studied morphologically ranged from subadult to adult (maximum total length of adults 68 cm males, 95 cm females, Compagno, 1984). Skeletal elements described include the scapulocoracoid, basals, and radials, while muscles described include the fin levator or adductor, fin depressor or abductor, fin protractor, epaxialis, hypaxialis, and cucullaris.

### Kinematics

Sharks were videotaped in a 600-l flow tank using a NAC HSV500c[3] two-camera high-speed video system at 250 fields $s^{-1}$ (downloaded image resolution $640 \times 480$ pixels for each camera) both while swimming in the water column and during benthic station-holding. The working area of the flow tank was 82 cm long $\times$ 28 cm wide $\times$ 28 cm high. Lateral and ventral views of sharks were recorded by directing one camera perpendicular to the side of the flow

tank and a second camera at a front-surface mirror oriented at a 45° degree angle below the working section of the tank. Lateral and ventral cameras were electronically synchronized and scaled using similarly marked grids. The head and pectoral region of sharks was recorded for detailed 3D analysis of pectoral fin conformation and body angle. Video sequences were digitized using a custom computer program as in previous research (Wilga and Lauder, 1999, 2000).

Sharks were filmed while holding position on the bottom of the flow tank at four flow speeds: 0.0, 0.5, 0.75, and 1.0 total lengths per second ($ls^{-1}$) to investigate whether body or fin movements change with flow speed. Five different sequences at four speeds in each of five individuals for a total of 100 images were digitized for the benthic speed effect experiments.

Steady horizontal swimming (pelagic holding position) at 1.0 $ls^{-1}$ was studied as the sharks swam in the flow tank. Rising and sinking locomotion in the water column were also studied to investigate whether the sharks alter the angle of the body or pectoral fins to change vertical position. We define holding position as the fish maintaining a stationary (within 2% $ls^{-1}$ deviation from a fixed reference point) horizontal (anteroposterior) and vertical position in the water column. Rising and sinking are defined as maintaining horizontal position in the water column while actively increasing or decreasing vertical position by at least 4 cm $s^{-1}$ with minimal lateral deviation. These criteria follow those we have used in previous studies (Wilga and Lauder, 1999, 2000). We analyzed only those video sequences in which sharks maintained horizontal and vertical position during holding or ascended or descended smoothly in the water column during rising and sinking (in all cases with minimal lateral, upstream–downstream, pitching, except when initiating changes in vertical position or roll motions). The initiation of rising and sinking behaviors necessarily involves pitching movements. A total of 300 images were digitized for these measurements of body and pectoral fin position during swimming: five fields equally spaced throughout a tailbeat for five tailbeats in four individuals for three behaviors. In order to minimize potential boundary effects from the tank walls on the flow around the fish for all experimental protocols, only sequences in which any body or pectoral fin surface of the shark was at least 4 cm from any side of the flow tank or surface of the water were analyzed (Webb, 1993).

The $x, y,$ and $z$ coordinates of 11 points were digitized on simultaneous lateral and ventral views of the head and pectoral fins (Fig. 1A,B): point 1, fixed reference mark on the background; 2, ventral body surface ventral to posterior margin of the eye; 3, anterior base of pectoral fin; 4, lateral pectoral fin tip; 5, posterior edge of pectoral fin; 6, internal marked location on fin surface; 7, anterior base of
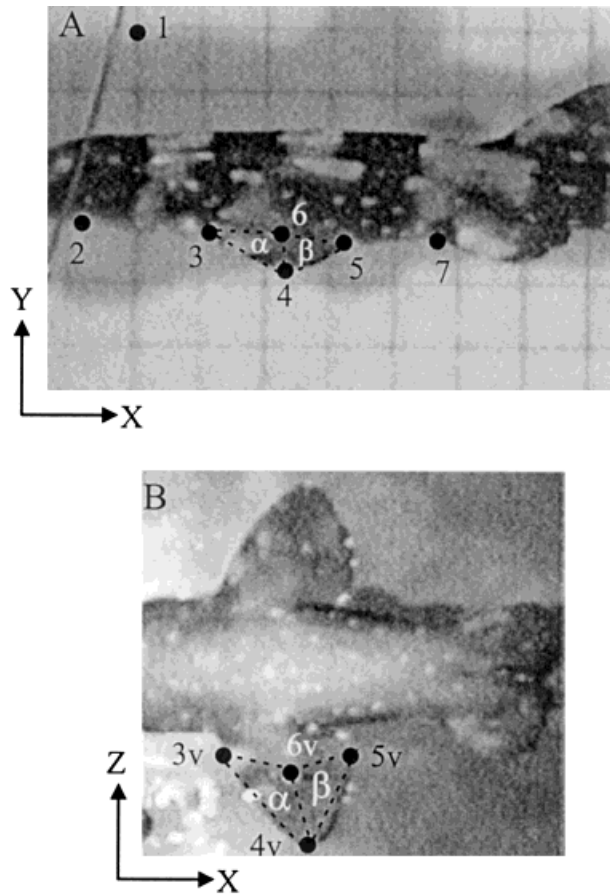
Fig. 1. Video images of a white-spotted bamboo shark, *Chiloscyllium plagiosum,* illustrating the points digitized on the body and pectoral fin. **A**: Lateral view of head and pectoral fin. **B**: Ventral view of pectoral fin region. Note that the reference axes differ for lateral (x, y) and ventral (x, z) views. Data in **A** and **B** were recorded simultaneously. Points 3 to 5 are the same points in lateral and ventral views, while points 6 and 6v represent the same location on the dorsal and ventral fin surfaces. These 3D coordinate data were used to calculate a 3D planar angle between the anterior and posterior fin planes (α and β) as shown in **A** and **B**, as well as to calculate the orientation of each fin plane relative to three external reference planes (*XY, XZ, YZ*; see Materials and Methods).

pelvic fin. On ventral images of the pectoral fins, the $x$ and $z$ coordinates of six points were digitized (Fig. 1B): 3v anterior base of pectoral fin; 4v, lateral fin tip; 5v, posterior fin margin; 6v, medial marked point on the fin.

Prior to filming the head and pectoral views, points 3–6 on the shark pectoral fins were marked to provide reliable landmarks for video digitizing. Reliable identification of specific points on the fin margins and interior is not possible without marking the fins. To mark pectoral fins, sharks were anesthetized using 0.15 gl$^{-1}$ tricaine methanesulfate (MS-222), intubated, and maintained on 0.065 gl$^{-1}$ while reflective aluminum markers were glued to the pectoral fins using cyanoacrylate adhesive following procedures used previously (Wilga and Lauder,

1999, 2000). Rectangular markers (0.5 × 0.2 cm) for points 3–5 and 3v–5v were wrapped around the edge of the fin so that they were visible in both lateral and ventral images. Small square markers (0.2 cm$^2$) for points 6 and 6v were glued to the dorsal and ventral surfaces of the fin. Preliminary video recordings were used to place points 6 and 6v at a position where the posterior portion of the fin begins to move vertically (as a flap) during rising and sinking behaviors. After the markers were glued in place, the sharks were intubated with fresh seawater until swimming movements began, after which animals were returned to the flow tank and allowed to recover for at least 3 h prior to video recording.

As in our previous articles (Wilga and Lauder, 1999, 2000) a 3D planar angle between the two triangles comprising the pectoral fin (Fig. 1: α, β) (animal frame of reference) was calculated as well as the angle that each of these triangles makes to three perpendicular reference planes (earth frame of reference). These angles were used to detect any change in the conformation and position of the pectoral fin surface among the three behaviors during locomotion and benthic station-holding. Examination of video tape sequences and digitized data showed that movement of the posterior region of the pectoral fin is well-represented by plane β and that movement of the entire surface of the pectoral fin is well-represented by quantifying the position of the two planes α and β.

The working space of the flow tank in which the sharks are placed can be divided into a standard Cartesian coordinate system where the position of any point in space can be identified by $x, y,$ and $z$ values (Fig. 1). The measurements and calculations follow the procedures used in our previous research (Ferry and Lauder, 1996; Lauder and Jayne, 1996; Wilga and Lauder, 1999, 2000). The lower left corner in the lateral view for the $x$ (horizontal) and $y$ (vertical) dimensions and the ventral view for the $x$ (horizontal) and $z$ (vertical) dimensions were defined as the origin of the coordinate system. The $x, y$ and $z$ coordinates for each point were obtained by using the $x$ and $y$ coordinates in horizontal view and the $z$ coordinate in ventral view with the redundant $x$ coordinate data in the ventral recording not used. Points 3, 3v, 4, 4v, and 6, 6v were used to form fin triangle α and points 4, 4v, 5, 5v, 6, 6v were used to form fin triangle β. The angle that triangles α and β make with the three orthogonal reference planes, parasagittal (*XY*), transverse (*YZ*), and frontal (*XZ*), was calculated by determining the orientation of the triangles in 3D space. The parasagittal plane is parallel to the longitudinal axis of the shark when swimming and is equivalent to the side of the flow tank (visible as the lateral camera view). The transverse plane is the plane toward which the shark is swimming and is represented as the front wall of the flow tank. The frontal plane is equivalent to the floor of the tank (visible as the ventral view). The planar

angle of intersection between fin triangles $\alpha$ and $\beta$ with each of the three reference planes was calculated from the $x, y,$ and $z$ coordinates and the coordinates of each of the three reference planes. The $XZ$ angle was measured using the convention that 0° and 180° represent upstream and downstream orientations within the reference plane, with angles greater than 180° indicating that the fin planes extend below the $XZ$ reference plane. Both $YZ$ and $XY$ planar angles were measured from dorsal to ventral with 0° dorsal and 180° ventral. $YZ$ angles greater than 90° thus indicate that pectoral fin planes are held at a positive angle of attack to the transverse plane with their upstream edge located dorsal to the downstream edge. $XY$ planar angles greater than 90° reflect an obtuse angle to the parasagittal plane and that the fin is inclined ventrally in a negative dihedral orientation.

## Digital Particle Image Velocimetry

Water flow in the wake of the pectoral fins of sharks during benthic station-holding, pelagic station-holding, and rising and sinking behaviors was analyzed using DPIV as in previous research (Drucker and Lauder, 1999; Wilga and Lauder, 1999, 2000; Lauder, 2000). Water in the flow tank was seeded with near-neutrally buoyant 12 mm diameter silver-coated hollow glass beads (density 1.3 g cm$^{-3}$; Potters Industries). A 5W argon-ion laser was focused into a 1–2 mm thick by 10 cm wide light sheet and oriented into a vertical configuration using mirrors. Particle movement in the water flow was visualized as light reflected by the beads and recorded using an NAC HSV 500c[3] two-camera high-speed video system at 250 fps. The flow tank described above was used to record the benthic and pelagic swimming sharks (for further details, see Wilga and Lauder, 1999, 2000). Water flow and particle reflections in the wake of the pectoral fin in lateral (parasagittal) view were recorded by placing one camera perpendicular to the side of the flow tank. The position of the shark relative to the laser light sheet in posterior (transverse) view was recorded by directing a second (synchronized) camera at the surface of a mirror placed in the flow at a distance of 30–40 cm behind the swimming shark and positioned 45° to the side of the flow tank. Previous studies have shown that the presence of the mirror does not affect the flow in the region of interest and imparts no statistical effects on locomotor kinematics (Ferry and Lauder, 1996; Drucker and Lauder, 1999; Wilga and Lauder, 1999, 2000).

Sequences of particle images during benthic and pelagic station-holding and rising and sinking in the water column in sharks were identified using the criteria described above for fin kinematics. Consecutive pairs of video images (4 ms apart) of the water flow just downstream of the pectoral fin were digitized and analyzed using two-frame cross-

correlation to produce a 20 × 20 matrix of 400 velocity vectors, as per conventional DPIV methods (Raffel et al., 1998; Lauder, 2000). A total of 48 image pairs was analyzed using DPIV: four occurrences each of pelagic station-holding at 1.0 $l$s$^{-1}$, benthic station-holding at 0.5 $l$s$^{-1}$, and benthic station-holding at 0.75 $l$s$^{-1}$ from three sharks; and three occurrences of rising in the water column and nine of sinking in the water column from two sharks. The DPIV estimation of mean velocity was within 5% of the true velocity by comparing the average free-stream velocity calculated using DPIV to that calculated by tracking individual particles (PTV) (Drucker and Lauder, 1999).

Rectangular subimages were used for the cross-correlation calculations of velocity vectors (Wilga and Lauder, 2000). Particles used for the cross-correlation analyses did not move more than 20% of the box width between the two frames in the relatively short time interval (4 ms) between images and the relatively slow flow velocities used in these experiments. Three analytical protocols were used to quantify water flow patterns in the wake of the pectoral fin for benthic and swimming sharks. First, fluid flow patterns in the wake of the fin were documented by estimating flow structure using the magnitude and direction of velocity vectors from plots of the 20 × 20 matrix of velocity vectors. Flow tank current was subtracted from the matrix of velocity vectors in order to reveal fluid structures in the wake.

Second, fluid vorticity was calculated by quantifying rotational motion in the flow using the velocity vector matrix. Plots of vorticity are shown in order to visualize rotational fluid motion in which greenish color indicates zero vorticity, red/orange color is used for counterclockwise fluid movement, and purple/blue color for clockwise motion (Krothapalli et al., 1997; Drucker and Lauder, 1999; Wilga and Lauder, 1999, 2000).

Third, a 2D estimate of lift force generated by the pectoral fin was computed from the velocity vector matrix. Lift forces generated by the pectoral fin were calculated from the circulation of vortices shed from the trailing edge of the fin. According to Kelvin's Law, shed vortices are of equal and opposite strength to the bound circulation on the fin (Dickinson, 1996). Therefore, the circulation ($\Gamma$, cm$^2$s$^{-1}$) of vortices shed by the pectoral fins was calculated from the matrix of velocity vectors using a custom program to estimate the bound circulation on the fin as done previously (Drucker and Lauder, 1999; Wilga and Lauder, 1999, 2000). The circular integration area $C$ around a vortex center is defined interactively using the matrix of velocity vectors. Linear interpolation of the four adjoining neighboring vectors in the matrix was used to calculate velocities at points on $C$ and by summing the tangential components around $C$ until an asymptotic value for total vortex circulation was detected by calculat-

ing increasing integration of path radii at 0.01 cm increments. Lift force (N) exerted by the pectoral fin on the water was calculated in two dimensions using $F = 2mt^{-1}$ (Dickinson, 1996), where 2 represents the force generated by both fins, m is fluid impulse, and t is the duration of pectoral fin movement digitized from video sequences. Fluid impulse ($kgms^{-1}$) was quantified using $m = \rho\Gamma A$, at a density of 1250 ($\rho$, $kgm^{-3}$), and A for the cross-sectional area ($cm^2$) of the vortex calculated using $\pi r^2$ where r is the digitized radius of the vortex ring. Vortices in the wake of the fin were typically observed following movement of the posterior region of the pectoral fin (triangle β) during rising and sinking behaviors and as they rolled off the stationary fin during benthic holding.

Since lift forces were calculated using fluid momentum data obtained from the 2D laser light sheet, these calculations permit comparative analysis of fluid flow properties and lift force among the behaviors only, and do not constitute *total* lift force on the fin, for which 3D data are required (Drucker and Lauder, 1999; Wilga and Lauder, 1999).

## Statistical Tests

Linear regression analyses were calculated using 3D pectoral fin angle and body angle and adjusted $R^2$ values. For the body and pectoral fin variables vs. behavior analyses, a mixed-model two-way analysis of variance (ANOVA) using Type III sums of squares was performed (Hicks, 1982) (SAS, Cary, NC). Behavior was treated as a fixed main effect and individuals as a random main effect, and consequently behavior was tested over the behavior $\times$ individual interaction term. If a difference was detected by ANOVA, then a post-hoc Student-Newman-Keuls (SNK) multiple comparisons test was performed. Data were tested for homogenous variances using the Levene Median test ($P < 0.05$) and normal distribution using the Kolmogorov-Smirnov test ($P < 0.05$). Statistical tests were performed using SAS v. 6.12 or SigmaStat v. 2.01 statistical software or calculated using Zar (1996).

## RESULTS
## Morphology

The skeletal and muscular anatomy of the pectoral girdle of white-spotted bamboo sharks, *Chiloscyllium plagiosum*, is illustrated in Figure 2. The pectoral girdle or scapulocoracoid cartilage is composed of fused coracoid and scapular cartilages. The medial portion of the scapulocoracoid cartilage is the coracoid bar, which extends anteromedially to meet its antimere at the midline. The scapular process extends posterodorsally from the lateral end of the coracoid bar. The pectoral fin skeleton is composed of three basal cartilages, three rows of radial cartilages, and numerous fin rays. The basal cartilages

consist of a propterygium, mesopterygium, and metapterygium from lateral to medial, respectively, and extend posterolaterally from the articular surfaces of the lateral end of the coracoid bar. The basal cartilages articulate with the lateral end of the coracoid bar. The distal end of the mesopterygium curves posteriorly toward the distal end of the metapterygium, separating the two elements along most of their length. One long row of radial cartilages extends from the distal ends of all three basal cartilages and is followed distally by two more rows of shorter rectangular radial cartilages. Numerous fin rays or ceratotrichia (composed of cartilage in Chondrichthyes rather than bone as in Osteichthyes) extend from the third row of radial cartilages into the distal web of the fin and represent the primary support for the distal half of the pectoral fin. The fin rays and radial cartilages are connected to each other and to the basal cartilages by the surrounding connective tissue.

The muscles of the pectoral fin that extend outward from the trunk include the adductor (levator), abductor (depressor), and protractor muscles. The fin adductor muscle originates from the ventral portion and posteroventral edge of the scapular process and fans out ventrolaterally and ventroposteriorly to insert onto the proximal end of the fin rays at the distal end of the second row of radials. The fin adductor muscle elevates the pectoral fin. The protractor muscle originates from the lateral edge of the coracoid bar and extends laterally to insert onto the anteroventral edge of the propterygium. The protractor muscle pulls the pectoral fin anteriorly. The fin abductor muscle originates from the ventrolateral edge of the coracoid bar and fans out laterally and posteriorly to insert onto the proximal end of the fin rays at the distal end of the second row of radials. Contraction of the fin abductor muscle depresses the pectoral fin.

The muscles associated with the pectoral girdle that are contained within the trunk (i.e., do not extend into the fin) include the cucullaris, epaxialis, and hypaxialis. The cucullaris originates from the anterodorsal edge of the scapular process and extends anterodorsally to insert onto the lateral-most edge of the epaxialis musculature. The cucullaris may assist in respiratory movements as well as protracting the scapula. The epaxialis extends anteriorly to insert onto the occipital region of the chondrocranium. The epaxialis elevates the head. The hypaxialis extends anteriorly to insert onto the posterior edges of the scapular process and coracoid bar. A thickened region of hypaxialis musculature inserts on the posterior edge of the scapular process just dorsal to the fin adductor muscle. In this region, the hypaxialis rotates the scapula posteriorly, possibly assisting girdle rotation during submerged walking and digging and may stabilize the pectoral girdle when hypobranchial muscles such as the cora-
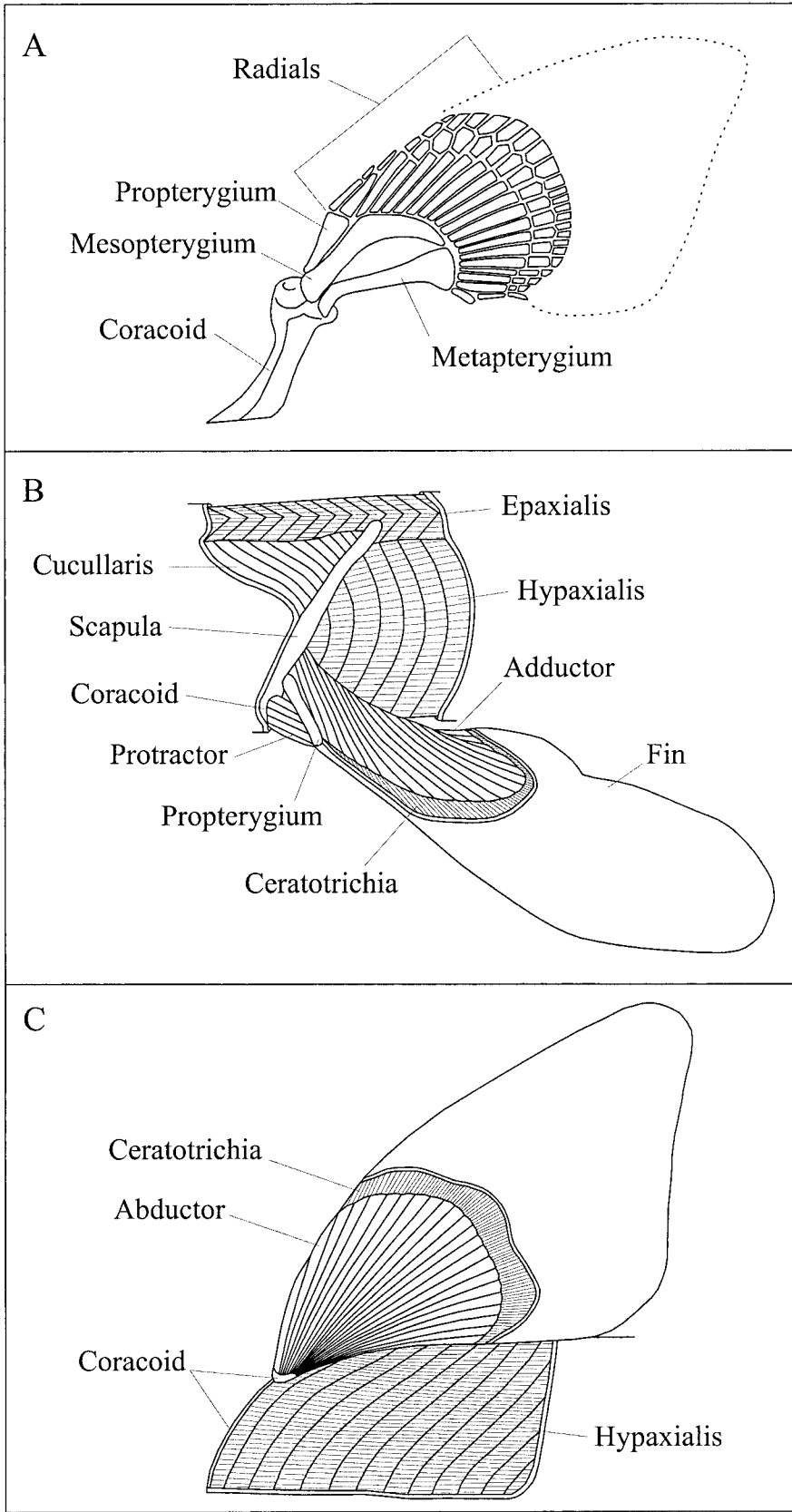
Fig. 2. Ventral (**A**) view of the pectoral fin skeleton in spotted bamboo sharks, *Chiloscyllium plagiosum*. Lateral (**B**) and ventral (**C**) views of the musculature of the pectoral fin region. Gray shading indicates skeletal elements. Dotted outline delimits the fin margin.

TABLE 1. *Summary means of kinematic variables and lift force in* Chiloscyllium plagiosum *during benthic station-holding at various speeds (ls$^{-1}$)*

| Variable | 0 | 0.5 | 0.75 | 1.0 | P value | SNK |
|---|---|---|---|---|---|---|
| Body tilt angle relative to flow (°) | 4.0 (0.58) | 3.3 (0.63) | 1.7 (0.50) | 0.6 (0.40) | 0.001* | 0, 0.5 > 0.75 > 1.0 |
| Pectoral fin angle ($\alpha$ to $\beta$ plane, °) | 174 (1.41) | 167 (2.42) | 165 (1.79) | 165 (1.61) | 0.001* | 0 > 0.5, 0.75, 1.0 |
| Pectoral fin chord angle to flow (°) | 2.7 (0.95) | −0.5 (1.09) | −2.74 (0.66) | −3.9 (0.82) | 0.006* | 0 > 0.5 > 0.75, 1.0 |
| Lift force (N) | — | −0.064 (0.0124) | −0.084 (0.0102) | — | 0.1820 | |

Values are means (standard error) for five sequences in each of five individuals.
*Significant at the Bonferroni corrected P value of 0.0125.
Angles are in degrees. No forces were calculated at 0 and 1.0 $ls^{-1}$.

comandibularis are activated (Wilga and Motta, 1998a,b; Wilga et al., 2000).

## Benthic Station-Holding

Sharks oriented the longitudinal body axis to the flow at all flow speeds above 0 $ls^{-1}$. At 0 $ls^{-1}$, sharks did not orient to the flow. Sharks maintained position on the bottom of the flow tank up to speeds of 1.0 $ls^{-1}$, at which speed some individuals started to slip backwards after holding position for a short time. The angle of the body relative to the flow significantly decreased from a mean of 4.0° at 0 $ls^{-1}$ to 0.6° at 1.0 $ls^{-1}$ (Table 1; ANOVA, $P = 0.001$).

Conformation of the pectoral fin surface changed significantly from 0 to 1.0 $ls^{-1}$ as revealed by 3D analyses of the pectoral fin angles (Fig. 3; ANOVA,

$P = 0.001$). The pectoral fin was held at a mean internal angle of 174° between planes $\alpha$ and $\beta$ at 0 $ls^{-1}$, indicating that the fin is maintained in a concave *upward* orientation (Fig. 3). The internal angle of the pectoral fin decreased to a mean of 165° in moving flow from 0.50 to 1.0 $ls^{-1}$ (Table 1). If the internal angle were 180°, $\alpha$ and $\beta$ would be coplanar and the fin would be held like a rigid flat plate.

Pectoral fin plane $\alpha$ was held outward from the body at a mean angle of 98.5° (Table 2) from the parasagittal (*XY*) plane while holding position on the substrate at all flow speeds. The leading fin edge is slightly dorsal to the trailing edge with the fin chord inclined at a 2.7° angle to the flow in still water (0 $ls^{-1}$) (Table 2). The angle of attack of the pectoral fin considered as a whole is thus *positive* in still water, with the lateral tip of the fin slightly
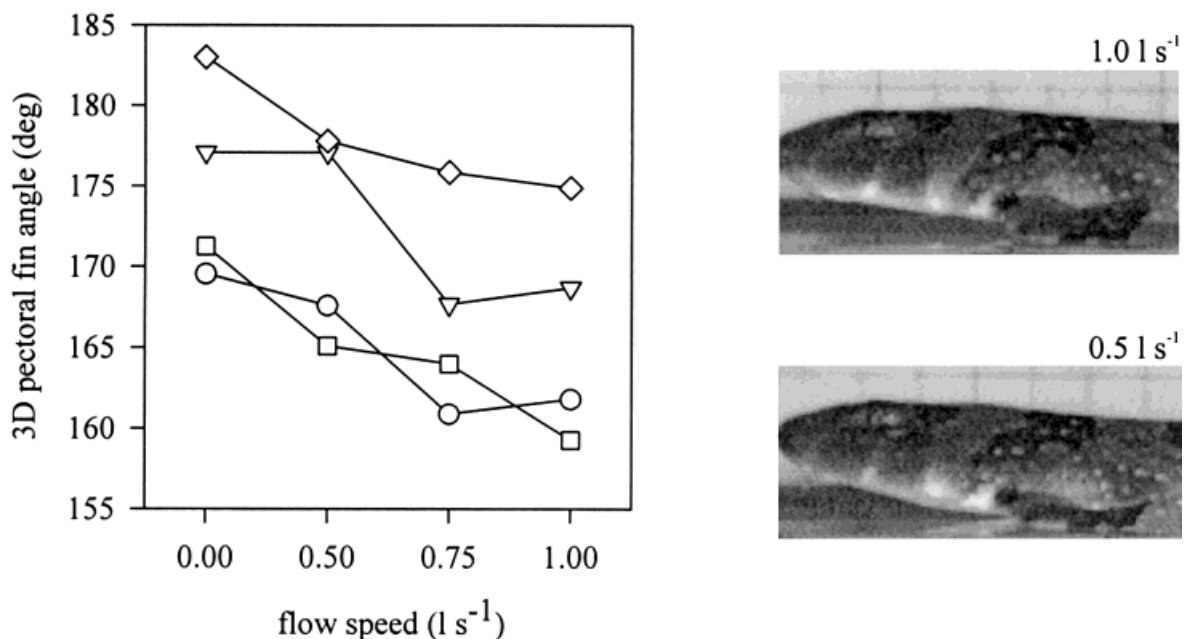


Fig. 3. Plot of 3D internal pectoral fin angle vs. flow speed during benthic holding station in *Chiloscyllium plagiosum*. Each symbol represents the mean of five body angle measurements (equally spaced in time) for five tailbeats for four individuals. Images on the right show head and pectoral fin conformation at 0.5 and 1.0 $ls^{-1}$ (flow direction is left to right). At all speeds sharks are maintaining position on the substrate. Three-dimensional internal pectoral fin angle is significantly different during flow speeds than in still water (ANOVA, $P = 0.001$).

　　　　　　　　　　　　　C.D. WILGA AND G.V. LAUDER

*TABLE 2. Summary statistics of 3D planar angles (degrees) for the pectoral fin of* Chiloscyllium plagiosum *while holding station on the substrate at increasing flow speed*

| Plane | Triangle | 0 | 0.5 | 0.75 | 1.0 | *P* value | SNK |
|---|---|---|---|---|---|---|---|
| *XZ* | α | 190 (1.01) | 190 (1.69) | 187 (2.07) | 188 (1.55) | 0.554 | |
| *XZ* | β | 179 (2.42) | 173 (2.97) | 164 (0.94) | 163 (1.11) | 0.003* | 0 > 0.5 > 0.75, 1.0 |
| *YZ* | α | 96 (0.92) | 96 (1.30) | 95 (1.04) | 94 (0.78) | 0.606 | |
| *YZ* | β | 90 (1.55) | 84 (1.89) | 81 (1.09) | 79 (1.38) | 0.0001* | 0 > 0.5 > 0.75, 1.0 |
| *XY* | α | 98 (0.89) | 98 (0.65) | 99 (0.66) | 99 (0.49) | 0.241 | |
| *XY* | β | 98 (0.41) | 101 (0.80) | 102 (0.52) | 102 (0.56) | 0.004* | 0 < 0.5, 0.75, 1.0 |

Values are means (standard error) for five sequences in each of five individuals.
*Significant at the Bonferroni corrected *P* value of 0.008.
In the *XZ* plane (floor of tank) 0° is anterior and 180° is posterior; in the *YZ* (anterior side of tank toward which the shark is facing) and *ZY* (back side of tank to the right of the shark) planes 0° is dorsal and 180° is ventral. Note that the orientation of the β triangle to the perpendicular of the *YZ* plane represents the plane of the posterior portion of the pectoral fin relative to the flow.

ventral to the base and posterior margin of the fin. The posterior plane (β) of the pectoral fin significantly changes orientation to the three reference planes at flow speeds from 0.75 to 1.0 $ls^{-1}$ (Table 2). The angle of pectoral fin plane β to the parasagittal (*XY*) plane increases to 102° (12° below horizontal), increasing the angle to the flow to about 180° as measured to the transverse plane (*YZ*), and by about 163° to the frontal plane (Table 2). The angle of attack of the pectoral fin thus changes to *negative* in flowing water (−0.50° at 0.5 $ls^{-1}$, -2.5° at 0.75 $ls^{-1}$ and −3.93° at 1.0 $ls^{-1}$) with the lateral tip of the fin significantly ventral to the base and posterior margin of the fin.

DPIV was used to visualize the pattern of water flow in the wake of the pectoral fin while holding station on the substrate. Calculated velocity vectors were superimposed on corresponding video images and a representative sequence is shown for benthic station-holding in Figure 4. The body of the shark was often faintly seen through the light sheet while the left pectoral fin was clearly visible as it extended through (or just anterior to) the light sheet and cast a vertical shadow by blocking laser light coming from below.

The DPIV analyses of bamboo sharks while station-holding on the substrate reveal that water flow is deflected upwards as it comes over the top of
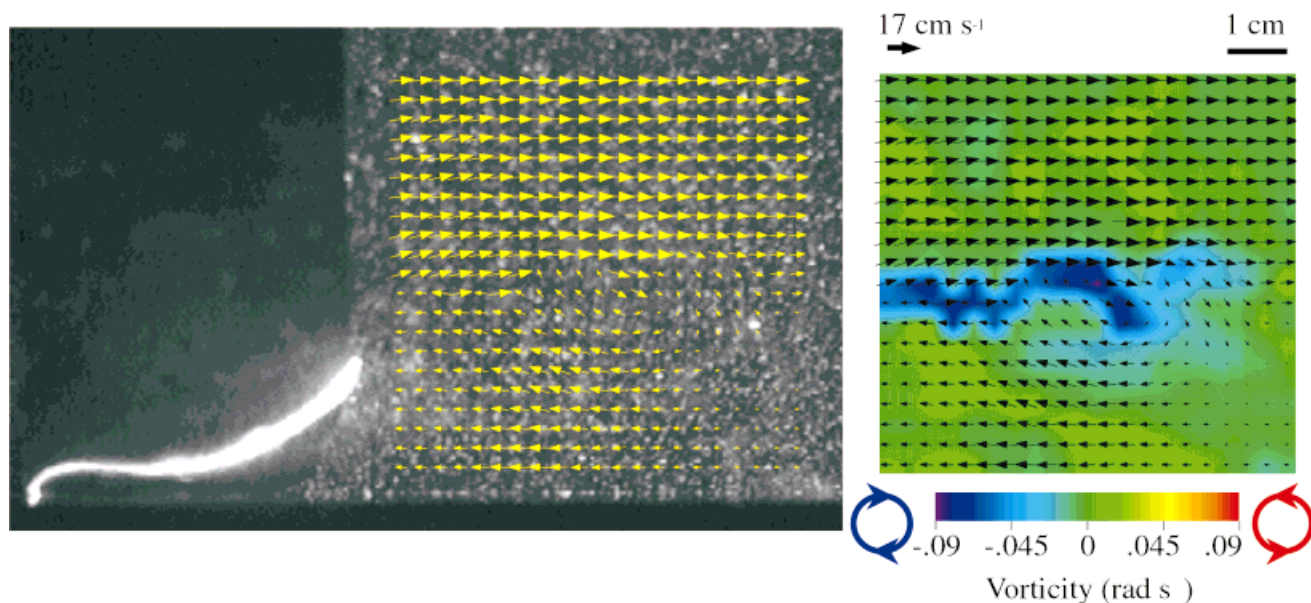


Fig. 4. DPIV data from the pectoral fins of *Chiloscyllium plagiosum* while holding station on the substrate. Video image (on left) shows a shark with the left pectoral fin located in the anterior end of the laser light sheet. The 20 × 20 matrix of yellow vectors downstream of the pectoral fin represents the results of DPIV calculations based on particle images visible as the speckled pattern in the light sheet. Note that the fin is held at a negative chord angle to the flow. The plot on the right shows fluid vorticity with superimposed velocity vectors (scaled to the same size as the vector matrix in the video image). A clockwise vortex (negative vorticity) was produced in the wake of the pectoral fins, which continues to rotate just behind the fin for several seconds until it is carried downstream by the flow (as seen here), after which a new vortex will form in the wake of the fin. Note that green color indicates no fluid rotation, blue color reflects clockwise fluid rotation, and red/yellow color indicates counterclockwise fluid rotation.
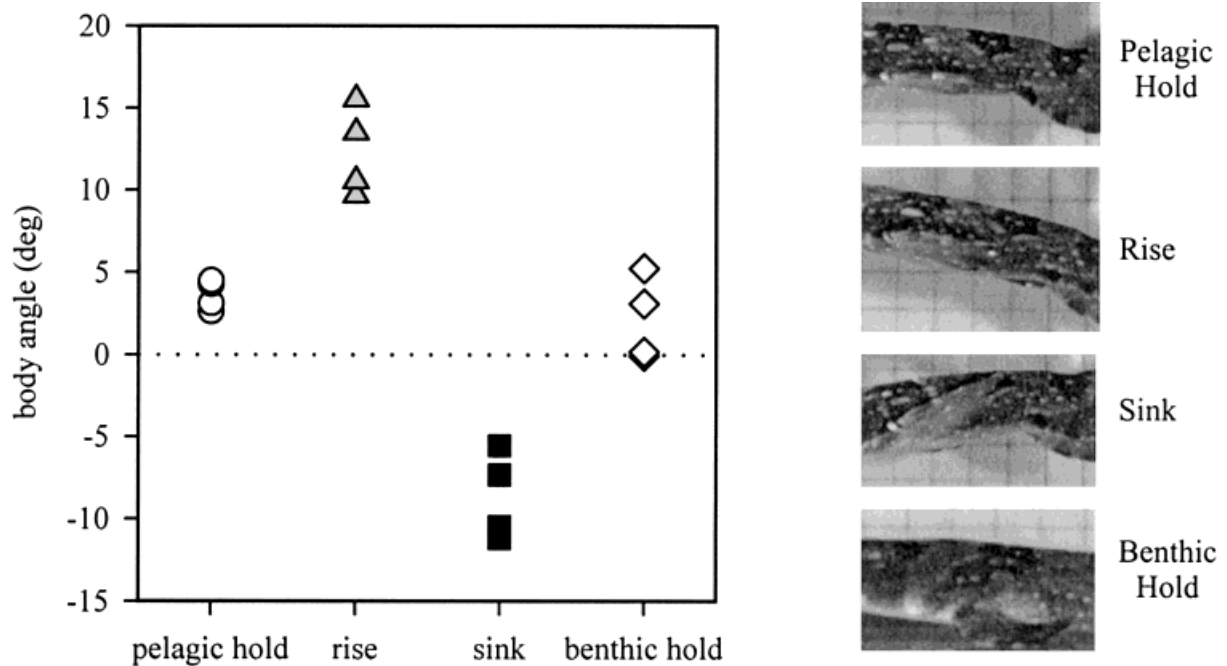
Fig. 5. Plot of body angle vs. behavior during locomotion in *Chiloscyllium plagiosum*. Circles indicate holding behavior, triangles show rising behavior, and squares reflect sinking behavior, all at 1.0 $ls^{-1}$. Body angle was calculated using the line connecting points 2 and 7 (Fig. 1) and the horizontal (parallel to the flow). Each point represents the mean of five sequences for each of four individuals. Images to the right show a sample body position during pelagic hold, rise, sink, and benthic hold behaviors. Body angle is significantly different among the three behaviors (ANOVA, $P = 0.0001$).

the pectoral fin and then forms a clockwise vortex (negative vorticity) just behind the pectoral fin (Fig. 4). The vortex continues to rotate behind the fin for several seconds until the flow carries it downstream, after which a new vortex forms in the wake of the fin. As water rotates clockwise behind the pectoral fin, some fluid moves forward along the substrate toward the back of the fin (note the upstream pointing arrows in the lower left portion of the vector field in Fig. 4). Vortex shedding and upstream water flow behind the fin was observed at all flow speeds during benthic station-holding. Water above the fin is moving downstream in the free stream while flow near the substrate posteroventral to the pectoral fin is moving upstream.

Mean values for relative downstream vertical fluid impulse were calculated from the velocity vector matrix and from video images (Table 1). The clockwise vorticity observed in the wake of the pectoral fin during benthic station-holding corresponds to a negative lift force that acts to force the pectoral fins ventrally and is significantly different from zero (mean lift at 0.5 and 0.75 $ls^{-1}$ = $-0.0732$ N; $t$-test $P < 0.001$).

## Pelagic Station-Holding and Maneuvering

Sharks held position in the flow tank using continuous undulations of the body and tail with the body at a positive tilt relative to the flow while swimming at 1.0 $ls^{-1}$ (Fig. 5). A positive body tilt averaging 3.6° was maintained while holding position. Sharks swam horizontally with no pitching or vertical or lateral drifting during holding sequences.

The conformation of the pectoral fin does not change throughout the tail-beat cycle while holding. During holding behavior, the pectoral fin is held at a mean internal angle of 190° (Table 3) between planes α and β, indicating that the fin is held at a slightly concave *downward* orientation. Pectoral fin plane α was held outward from the body at a mean angle of 96° (Table 4) from the parasagittal (*XY*) plane while holding position. The leading fin edge is dorsal to the trailing edge, with the fin chord inclined at a 4° angle to the flow (Fig. 7A). The angle of attack of the pectoral fin is thus *positive* during holding position and the lateral tip of the fin is significantly ventral to the base and posterior margin of the fin.

Sharks smoothly rose or sank (instead of rolling or yawing) during the rise and sink sequences. Rising and sinking sequences were initiated by pitching movements caused by changes in pectoral fin angle, as described below. The angle of the body relative to the flow varied significantly while changing position in the water column at 1.0 $ls^{-1}$ (ANOVA, $P = 0.0001$) (Fig. 5). Sharks assumed a mean positive body tilt of 12.0° during rising and a mean negative body tilt of $-8.6°$ during sinking.

TABLE 3. *Summary means of kinematic variables and lift force in* Chiloscyllium plagiosum *while holding and changing position in the water column, compared to benthic station-holding*

| Variable | Hold | Rise | Sink | Benthic | P value | SNK |
|---|---|---|---|---|---|---|
| Body tilt angle relative to flow (°) | 3.6 (0.35) | 12 (0.97) | −8.6 (1.41) | 2.2 (0.51) | 0.0001* | R > H > B > S |
| Pectoral fin angle (α to β plane; °) | 190 (1.42) | 203 (2.50) | 178 (1.73) | 165 (2.13) | 0.0001* | R > H > S > B |
| Pectoral fin chord angle to flow (°) | 4 (0.54) | 20 (1.43) | −14 (2.12) | −2.5 (0.79) | 0.0001* | R > H > B > S |
| Lift force (N) | −0.0006 (0.00125) | 0.0125 (0.0044) | −0.0101 (±0.0019) | −0.084 (0.0102) | 0.0001* | B > H |

Values are means (standard error) for five sequences in each of four individuals.
*Significant at the Bonferroni corrected $P$ value of 0.0125.
B, benthic hold; H, pelagic hold; R, rise; S, sink. Pelagic holds, rises and sinks are at 1.0 $ls^{-1}$ and benthic holds are at 0.75 $ls^{-1}$; Lift force for benthic and pelagic holds only were statistically compared due to an insufficient number of DPIV sequences for rises and sinks.

During rising, the pectoral fin tilts so that the leading edge is even more dorsal to the trailing edge and the fin chord is at a positive 20° to the flow (Fig. 5, Table 3). The orientation of the pectoral fin during sinking changes significantly from that during holding with respect to all three reference planes (Fig. 5, Table 3). The lateral edge of the pectoral fin is more dorsally located, the posterior plane of the fin slants upward relative to the base, and the fin chord is oriented at a -14° angle to the flow (Fig. 5).

Conformation of the pectoral fin surface also changes significantly during the initiation of sinking and rising from an initial holding position at 1.0 $ls^{-1}$ (ANOVA, $P = 0.0001$; linear regression, pectoral fin angle = 188.387 + 0.926x, $R^2 = 0.440$, $P < 0.001$; Fig. 6). The internal angle increases to an average of 203° during rising (Table 3), indicating that the fin is held in an even greater concave down position, while the fin is concave upwards with a mean internal angle of 178° during sinking. The change of internal angle is reflected by the repositioning of the pectoral fin to redirect water flow in order to reorient the body for rising and sinking behaviors. Changes in internal pectoral fin angle precede the change in body angle associated with a rise or sink and function to initiate the pitching moment that reorients the body angle from the holding position to the more

extreme body angles associated with rising and sinking behavior (Fig. 5). Overall mean tailbeat duration was 309 ms, within which sharks actively increased or decreased vertical position by an average of 5.14 cm s$^{-1}$ during rising and 9.18 cm s$^{-1}$ during sinking.

During steady horizontal swimming in the water column, the DPIV analyses reveal downstream-oriented vectors and largely solid green vorticity fields, indicating that essentially no vorticity was detected in the wake of the pectoral fins of bamboo sharks (Fig. 8). In contrast, as bamboo sharks rose in the water column the downward flipping of the posterior portion of the pectoral fin generated a counterclockwise vortex that was shed from the trailing edge of the fin and initiated the upward pitching of the body. Similarly, a clockwise vortex (negative vorticity) was produced as the posterior portion of the pectoral fin flipped upward to initiate a sinking event.

Mean lift force values quantified during holding position in the water column were not significantly different from zero (mean lift = -0.0006 N; $t$-test $P = 0.098$). Lift forces produced by the pectoral fin are significantly different among the three behaviors (ANOVA, $P = 0.0001$). The clockwise vorticity observed in the wake of the pectoral fin during sinking

TABLE 4. *Summary statistics of 3D planar angles (degrees) for the pectoral fin of* Chiloscyllium plagiosum *while holding and changing position in the water column, compared to benthic station-holding*

| Plane | Triangle | Hold | Rise | Sink | Benthic | P value | SNK |
|---|---|---|---|---|---|---|---|
| XZ | α | 177 (3.26) | 206 (1.92) | 151 (1.87) | 187 (2.60) | 0.0001* | R > B > H > S |
| XZ | β | 195 (1.16) | 214 (1.88) | 155 (1.70) | 164 (1.11) | 0.0001* | R > H > B > S |
| YZ | α | 90 (0.72) | 105 (1.25) | 71 (2.17) | 94 (1.28) | 0.0001* | R > B > H > S |
| YZ | β | 99 (0.81) | 117 (1.64) | 75 (2.05) | 81 (1.28) | 0.0001* | R > H > B > S |
| XY | α | 96 (2.64) | 104 (3.40) | 79 (3.51) | 99 (0.77) | 0.0027* | R, B > H, B > S |
| XY | β | 91 (2.74) | 96 (3.70) | 77 (3.44) | 102 (0.62) | 0.0006* | R, B > H, B > S |

Values are means (standard error).
*Significant at the Bonferroni corrected $P$ value of 0.008.
B, benthic hold; H, pelagic hold; R, rise; S, sink. In the XZ plane (floor of tank) 0° is anterior and 180° is posterior; in the YZ (anterior side of tank toward which the shark is facing) and XY (back side of tank to the right of the shark) planes 0° is dorsal and 180° is ventral. Note that the orientation of the β triangle to the perpendicular of the YZ plane represents the plane of the posterior portion of the pectoral fin relative to the flow. Pelagic holds, rises and sinks are at 1.0 $ls^{-1}$ and benthic holds are at 0.75 $ls^{-1}$.
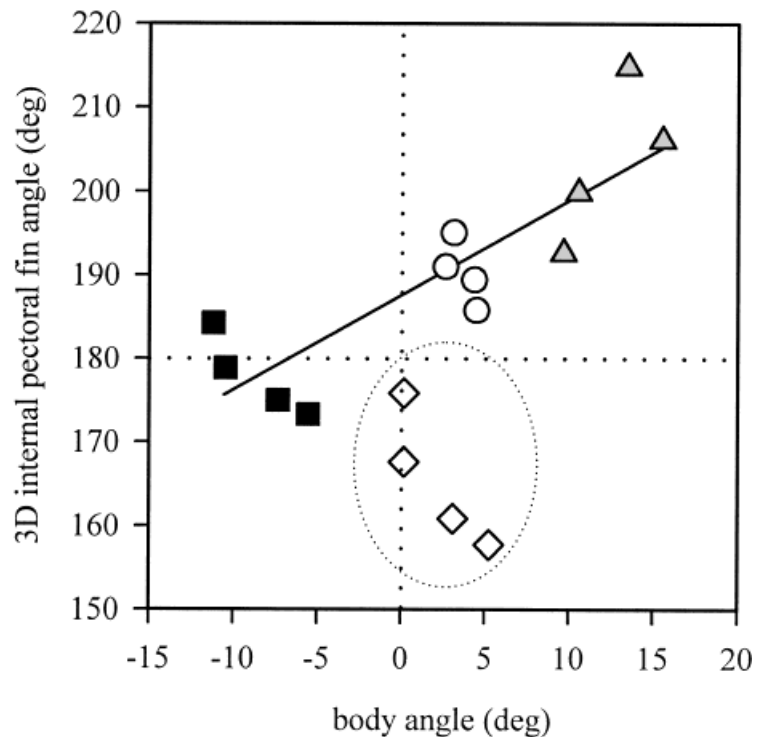
Fig. 6. Graph of 3D internal pectoral fin angle vs. body angle for pelagic and benthic holds, rises and sinks in *Chiloscyllium plagiosum*. Symbols as in Figure 5. Body angle was calculated using the line connecting points 2 and 7 (see Fig. 1) and the horizontal (parallel to the flow). Each point represents the mean of five sequences for each of four individuals. Pectoral fin angles equal to 180° indicate that the two fin triangles are co-planar; angles less than 180° show that the fin surface is concave dorsally; angles greater than 180° indicate that the fin surface is concave ventrally. The 3D internal pectoral fin angle is significantly different among the four behaviors (ANOVA, $P = 0.0001$). The least-squares regression line is significant (pectoral fin angle $= 188.387 + 0.926x$, adjusted $R^2 = 0.44$, $P < 0.001$). The regression line does not include benthic holding data which are enclosed by the dotted circle.

corresponds to a negative lift force that acts to pitch the body downwards and is significantly different from zero (mean lift $= -0.0101$ N; $t$-test $P < 0.001$). Similarly, counterclockwise vorticity observed in the wake of the pectoral fin during rising corresponds to a significant positive lift force that acts to pitch the body upwards (mean lift $= 0.0125$ N; $t$-test $P < 0.025$). Interestingly, negative lift during benthic station-holding is more than eight times higher than the negative lift forces recorded during sinking (mean lift $= -0.084$ N; $t$-test $P < 0.0001$) (Table 3).

## DISCUSSION
### Anatomy

The morphology of the pectoral fin in bamboo sharks, *Chiloscyllium plagiosum*, appears to allow great flexibility about the anteroposterior axis. The two relatively short rows of distal radials following the long proximal row permit bending at the level of the second and third rows to occur along a relatively small strip across the fin. Bamboo sharks commonly rest on the bottom with their head and trunk propped off the substrate by resting on the depressed and bent pectoral fins. In this posture, the basals and proximal radials are elevated off the substrate while the distal radials contact the substrate and bear the weight of the fish. When winnowing (digging) through gravel and backing up, only the distal portion of the pectoral fin (containing the fin rays) makes contact with the substrate. We commonly observed bamboo sharks engaged in sub-

merged walking similar to that reported in epaulette sharks, *Hemiscyllium ocellatum* (Pridmore, 1995), in which both sets of paired fins were used to walk on the substrate in a gait similar to a trot.

Pectoral fin structure varies greatly among shark species (Compagno, 1988). In bamboo sharks, the radials extend about 40–50% into the fin with the distal fin web supported only by fin rays (Fig. 9). The radials are parallel, articulate with each other, and have truncated distal tips. The relative lengths of the radials vary greatly among species, with the intermediate row usually shorter than the proximal row and the longest distal segment varying from less than half to twice that of the proximal segments (Compagno, 1988). The number of rows of radials also varies among species. In nurse sharks, *Ginglymostoma cirratum* (Orectolobiformes), the proximal row is similar in length to the four to five distal rows, while in bamboo sharks, *Chiloscyllium plagiosum*, the proximal row is much longer than the two distal rows, and in leopard sharks, *Triakis semifasciata*, the intermediate row is shorter than the proximal row with the distal row varying from 0.14–1.1 the length of the proximal row (Fig. 9; Dingerkus, 1986). Greater numbers of relatively shorter intermediate and distal segments may allow for increased flexibility of the pectoral fin surface and may promote maneuverability.

Bamboo sharks, *Chiloscyllium plagiosum*, appear to have greater pectoral flexibility compared to leopard sharks, *Triakis semifasciata*, during locomotion. The intraplanar angle of the pectoral fin ranged
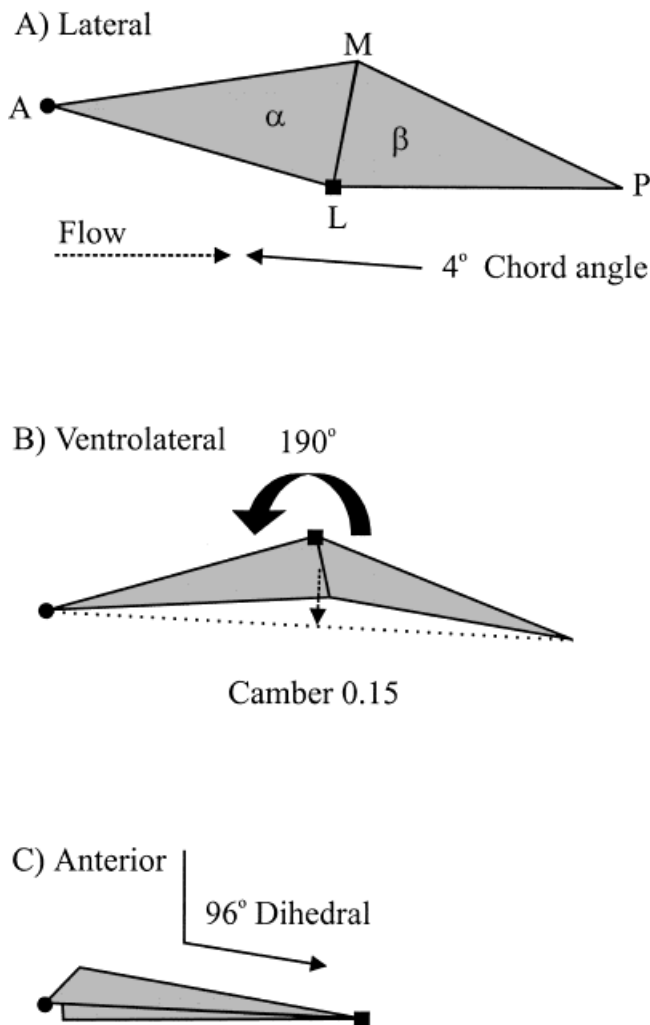
## A) Lateral



## B) Ventrolateral          190°



Camber 0.15

## C) Anterior



Fig. 7.   Orientation of the two pectoral fin planes (α and β) in 3D space during pelagic holding in *Chiloscyllium plagiosum*. Panels show (**A**) lateral, (**B**) ventrolateral, and (**C**) posterior views of the fin planes, respectively. Points defining the fin triangles correspond to the following digitized locations in Figure 1: A for anterior represents point 3, also indicated by black circle; L for lateral represents point 4, also indicated by black square; P for posterior represents point 5; M for medial represents point 6. Chord angle to the flow is given in the lateral view, camber and internal fin angle between planes β and β are given in the ventrolateral view, and the dihedral angle is shown in the posterior view (note that in the posterior view the angles are given as acute to the *XY* plane and thus are the complement to the angles reported in Table 4).

from a minimum of 163° (concave up) to a maximum of 203° (concave down) during locomotion in *C. plagiosum* (Table 3). Planar angles less than 163° during propping behavior and far exceeding 203° are attained during winnowing and backing up, but these behaviors were not quantified in this study. In contrast, the intraplanar angle of the pectoral fin in leopard sharks is never concave upwards in orientation during locomotion (Wilga and Lauder, 2000). Leopard shark fin angles ranged from 185–200° (Wilga and Lauder, 2000) (Table 1). We did not

observe leopard sharks propped up on the pectoral fins or engaging in submerged walking as in bamboo sharks.

It is unknown whether the intervening gap and associated musculature between the mesopterygium and metapterygium confer any functional advantages (Fig. 9). The dihedral and intraplanar angles encompass different planes than that containing the longitudinal axis of the basals, and thus differences between bamboo and leopard sharks in pectoral fin function associated with the gap are not captured by the present analysis. The muscle fibers in the gap are aligned longitudinally along the basals rather than running between them and are similar to the muscle fibers overlying non-gap regions of the basals. It is possible that the gap may permit increased bending between the two basals. A detailed 3D kinematic analysis consisting of fin triangles containing longitudinal planar elements of the pectoral fin for sharks containing the gap and lacking the gap, as well as an electromyographic analysis, are necessary to address the functional role of the basals and their associated musculature.

## Dynamics of Locomotion

In order to maintain position on the substrate during current flow, bamboo sharks shift their body posture to reduce drag, and adjust pectoral fin angle to generate negative lift, increase friction, and oppose downstream drag. Bamboo sharks oriented the longitudinal axis of the body to the flow with the head pointed upstream during current flow, but did not orient when current flow was absent. Plaice (*Pleuronectes platessa*), thornback skates (*Raja clavata*), sculpins (*Myoxocephalus scorpius*), and cod (*Gadus morhua*) also orient to the flow as flow velocity increases (Arnold, 1969; Arnold and Weihs, 1978; Webb, 1989; Gerstner, 1998; Gerstner and Webb, 1998). Body angle to the flow steadily decreases from 4° at 0 $ls^{-1}$, to 2.2 at 0.75 $ls^{-1}$, to 0.5° at 1.0 $ls^{-1}$ as bamboo sharks flatten their body against the substrate as flow speed increases. Station-holding Atlantic salmon parr, *Salmo salar*, and Atlantic cod, *G. morhua*, decrease body angle similarly as current flow velocity increases (Webb, 1989; Arnold et al., 1991). Flattening the body against the substrate reduces drag in higher current flows thereby promoting station-holding. This behavior is more advantageous to fusiform benthic fishes that experience a relatively high flow regime, such as streams where salmon parr are hatched (Webb, 1989) and inshore areas where bamboo sharks dwell (Compagno, 1984).

Bamboo sharks reorient the pectoral fins to generate negative lift and increase friction during station-holding in current flow. The concave upward orientation of the pectoral fin decreases from a mean planar angle of 174° at 0 $ls^{-1}$ to a mean of 165° at 1.0 $ls^{-1}$. At the same time, the chord angle of the pectoral
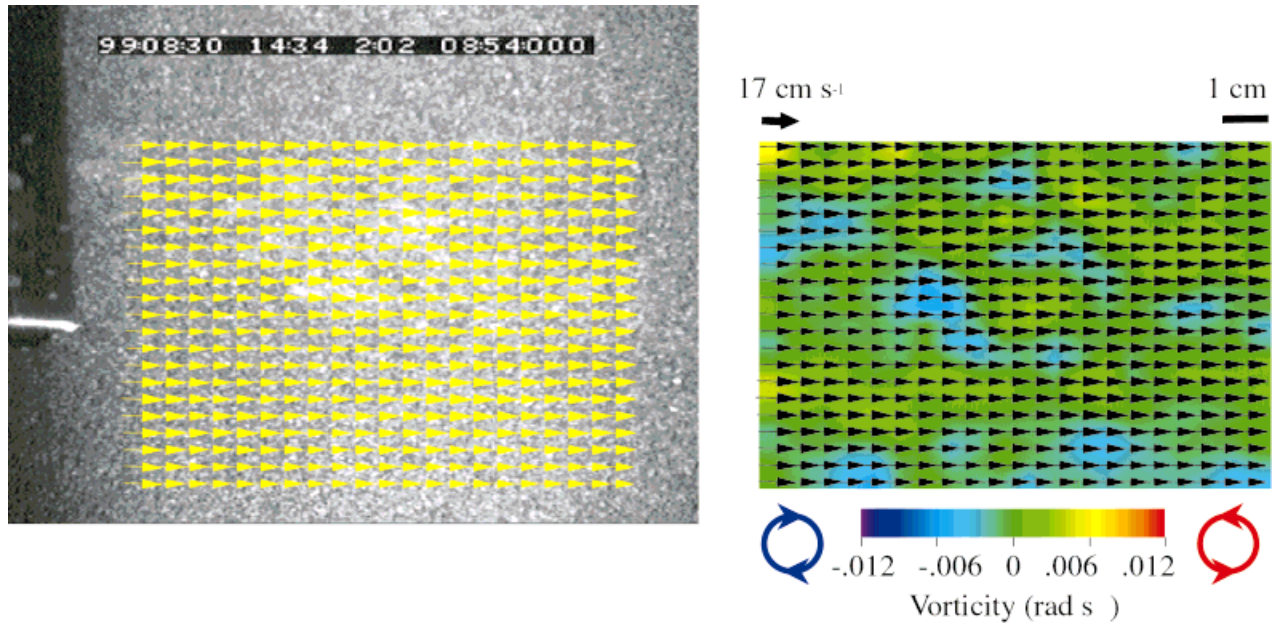
Fig. 8. DPIV data from the pectoral fins of *Chiloscyllium plagiosum* during pelagic holding behavior. Video image (on left) shows a single video image of a shark with the left pectoral fin located at the anterior edge of the laser light sheet. Note that the body is faintly visible through the light sheet. The $20 \times 20$ matrix of yellow vectors downstream of the pectoral fin represents the results of DPIV calculations based on particle images visible as the speckled pattern in the light sheet. The plot on the right shows fluid vorticity with superimposed velocity vectors (scaled to the same size as the vector matrix in the video image). Note that the fin is held in a slightly upwards position and that the vorticity plot shows effectively no fluid rotation. Hence, the pectoral fins in this position do not generate lift forces. Note that green color indicates no fluid rotation, blue color reflects clockwise fluid rotation, and red/yellow color indicates counterclockwise fluid rotation. To assist in visualizing the flow pattern, a mean horizontal flow of U = 20 cms$^{-1}$ was subtracted from each vector.

fin steadily decreases from a mean of 2.7° at 0 $ls^{-1}$ to a mean of –3.9° at 1.0 $ls^{-1}$. Flattening the body against the substrate lowers the anterior edge of the fin, while elevating the posterior edge of the fin to decrease the planar angle effectively decreases the chord angle. Posterior fin elevation is most likely actively controlled by activity of the adductor musculature (Fig. 2). The decreased chord and planar angle together act to deflect water up over the fin. Our DPIV analysis shows that as water is deflected upwards over the pectoral fin, a clockwise vortex is produced and shed from the fin tip. The clockwise vortex produces significant negative lift (mean –0.084 N) directed towards the substrate that is more than eight times the negative lift generated during open-water sinking behavior. The negative lift generated by the pectoral fin increases the total downward force on the fish and increases friction, which promotes station-holding.

Another interesting phenomenon is observed as bamboo sharks curl their fins while holding station in current flow. As the clockwise vortex shed from the fin rotates just behind the fin, flow is drawn upstream towards the posterior surface of the fin. This upstream flow pushes against the posterior surface of the pectoral fin and acts to oppose drag and promote station-holding. The fluid dynamic phenomena observed in station-holding bamboo sharks support previous proposals that the pectoral fins of

fishes during station-holding are oriented to generate negative lift (Arnold et al., 1991; Webb et al., 1996). Negative lift is directed toward the substrate in order to increase total downward force and friction force which promotes station-holding (Arnold et al., 1991; Webb et al., 1996). In addition, pectoral fin orientation of station-holding bamboo sharks results in a novel mechanism leading to vortex shedding that further aids benthic station-holding.

During station-holding in the water column the pectoral fins of bamboo sharks perform a very different function. There is no evidence of significant lift forces (mean –0.0006 N) in the wake of the pectoral fin during steady horizontal swimming in bamboo sharks. All flow behind the fin is oriented effectively downstream (Fig. 8) with no evidence of downward tilted vectors that would indicate downwash and the production of upward lift forces. This is similar to our previous findings of negligible lift generation by the pectoral fins during steady horizontal swimming in leopard sharks, *Triakis semifasciata*, and white sturgeon, *Acipenser transmontanus* (Wilga and Lauder, 1999, 2000), all of which were predicted to generate lift according to the classical theory of heterocercal tail locomotion (Affleck, 1950; Alexander, 1965; Simons, 1970; Thomson, 1976; Videler, 1993; Fish and Shannahan, 2000).

Bamboo sharks assume a body angle of 3.6° to the flow during steady horizontal swimming. The posi-
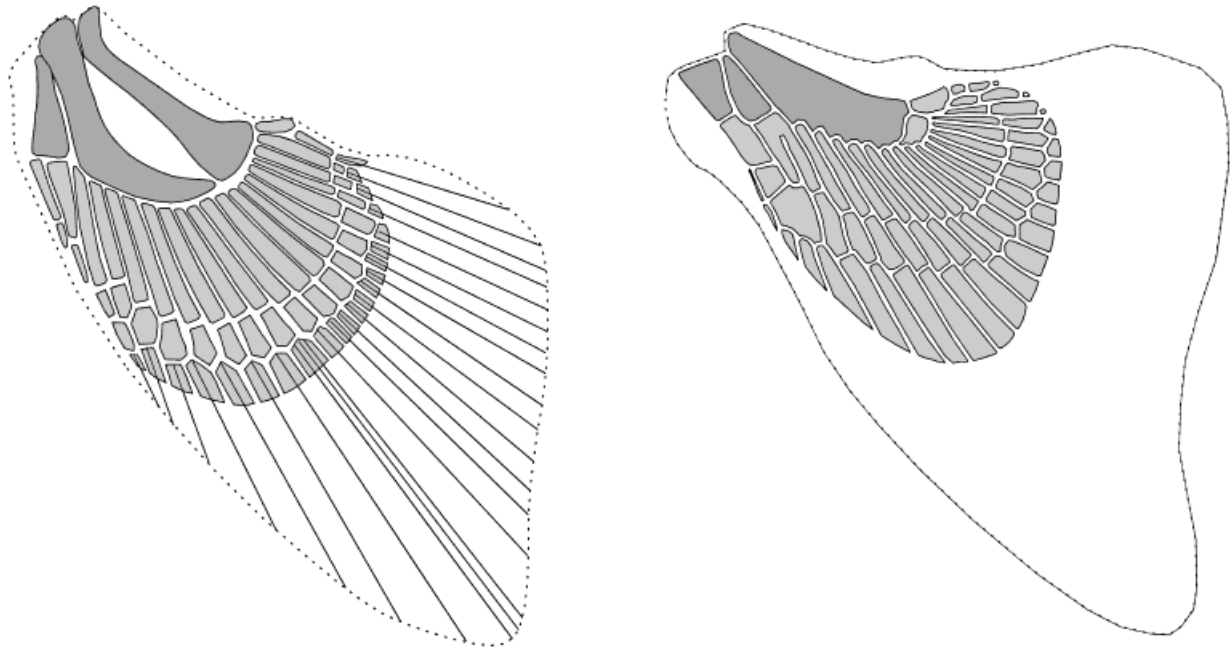
Fig. 9.   Skeletal structure of the pectoral fins in spotted bamboo sharks *Cephaloscyllium plagiosum* (left) and leopard sharks *Triakis semifasciata* (right) (adapted from Compagno, 1988). The left pectoral fin for each species is shown in dorsal view. Dark gray elements are propterygium, mesopterygium, and metapterygium from left to right; light gray elements are radials, dotted line delimits the fin margin.

tive body tilt indicates that upward lift may be generated by the ventral body surface, both anterior and posterior to the center of mass. This is also similar to leopard sharks, *Triakis semifasciata*, and white sturgeon, *Acipenser transmontanus*, which adopt a positive body angle to the flow during steady horizontal swimming that decreases with increasing flow speed (Wilga and Lauder, 1999, 2000). It has been suggested that negatively buoyant fishes, such as sharks and sturgeon, may assume a positive body tilt during steady horizontal swimming as a behavioral mechanism to increase the total body area generating lift (He and Wardle, 1986), and this appears to be the case for bamboo shark locomotion.

The 3D orientation of the pectoral fin in bamboo sharks during steady horizontal swimming is complex. The planar angle of the pectoral fin is concave downward (190°) in contrast to concave upward while station-holding on the substrate. Interestingly, the chord angle of the pectoral fin is 4.2°, suggesting that slight positive lift might be generated by the pectoral fins. However, negligible lift is generated as indicated by the DPIV analyses, and this is most likely due to the conformation of the pectoral fin (Fig. 7B) that is not a flat plate with a positive angle of attack. The pectoral fin is held at a negative dihedral angle of 6°, which promotes maneuverability rather than stability (Wilga and Lauder, 1999, 2000). Wings that are tilted at a positive angle to the horizontal have a positive dihedral angle (as seen in most airplanes) and are self-stabilizing in that they resist rolling

motions of the fuselage (Smith, 1992; Simons, 1994). In contrast, wings that are held at a negative dihedral are destabilizing and promote rolling motions of the fuselage. The dihedral angle in leopard sharks, *Triakis semifasciata* (-23°), and white sturgeon, *Acipenser transmontanus* (-33°) during steady horizontal swimming is much more negative than that in bamboo sharks (-6°), suggesting that sturgeon and leopard sharks are more unstable in roll during open-water swimming than bamboo sharks (Wilga and Lauder, 1999, 2000). It may be that benthic fishes, such as bamboo sharks, sacrifice maneuverability for stability when locomoting in the water column.

In order to complete the force balance on swimming bamboo sharks, data are needed on the direction of force generated by the tail during pelagic holding, sinking, and rising behaviors. Bamboo sharks possess a heterocercal tail, but with a substantially lower heterocercal angle than is found in most other sharks: the vertebral axis is much more horizontal as compared to leopard sharks (Ferry and Lauder, 1996; Wilga and Lauder, 2000) in which the dorsal tail lobe is at a substantial angle to the body axis. Variation in heterocercal tail morphology could potentially have a significant effect on the function of the tail during steady swimming in fishes. In leopard sharks the direction of force generated by the tail is directed anterodorsally due to the motion of the leading edge relative to the ventral portion of the fin (Ferry and Lauder, 1996). Bamboo sharks have a low heterocercal tail angle and therefore may

have different patterns of tail force generation with different effects on the overall force balance. Only DPIV analyses of caudal fin function in bamboo sharks will permit testing of this proposed correlation between heterocercal tail angle and the pattern of force production.

## ACKNOWLEDGMENTS

The authors thank Eliot Drucker, Stephen Anderson, Jimmy Liao, and Jen Nauen for providing assistance during the experiments and/or analysis. We also thank Eliot Drucker, Jimmy Liao, Frank Fish, and Jen Nauen for providing helpful comments or discussion during the course of this project. Oregon Coast Aquarium and Seaworld of San Diego generously donated the animals used in this project.

## LITERATURE CITED

Affleck RJ. 1950. Some points in the function, development, and evolution of the tail in fishes. Proc Zool Soc Lond 120:349–368.

Alexander RM. 1965. The lift produced by the heterocercal tails of Selachii. J Exp Biol 43:131–138.

Arnold GP. 1969. A flume for behaviour studies of marine fish. J Exp Biol 51:671–679.

Arnold GP, Weihs D. 1978. The hydrodynamics of rheotropism in the plaice (*Pleuronectes platessa* L.). J Exp Biol 75:147–169.

Arnold GP, Webb PW, Holdford BH. 1991. The role of the pectoral fins in station-holding of Atlantic salmon parr (*Salmo salar* L.). J Exp Biol 156:625–629.

Compagno LJV. 1984. Sharks of the world. Rome: United Nations Development Program.

Compagno LJV. 1988. Sharks of the order Carcharhiniformes. Princeton, NJ: Princeton University Press.

Dickinson MH. 1996. Unsteady mechanisms of force generation in aquatic and aerial locomotion. Am Zool 36:537–554.

Dingerkus G. 1986. Interrelationships of Orectolobiform sharks (Chondrichthyes: Selachii). Tokyo: Ichthyological Society of Japan.

Drucker EG, Lauder GV. 1999. Locomotor forces on a swimming fish: three-dimensional vortex wake dynamics quantified using digital particle image velocimetry. J Exp Biol 202:2393–2412.

Ferry LA, Lauder GV. 1996. Heterocercal tail function in leopard sharks: a three-dimensional kinematic analysis of two models. J Exp Biol 199:2253–2268.

Fish FE, Shannahan LD. 2000. The role of the pectoral fins in body trim of sharks. J Fish Biol 56:1062–1073.

Gerstner CL. 1998. Use of substratum ripples for flow refuging by Atlantic cod, *Gadus morhua*. Env Biol Fish 51:455–460.

Gerstner CL, Webb PW. 1998. The station-holding performance of the plaice *Pleuronectes platessa* on artificial substratum ripples. Can J Zool 76:260–268.

He P, Wardle CS. 1986. Tilting behavior of the Atlantic mackerel, *Scomber scombrus*, at low swimming speeds. J Fish Biol 29:223–232.

Hicks CR. 1982. Fundamental concepts in the design of experiments, 3rd ed. Orlando: Harcourt Brace Jovanovich College Publishers.

Jayne BC, Lauder GV. 1995. Are muscle fibers within fish myotomes activated synchronously? Patterns of recruitment within deep myomeric musculature during swimming in largemouth bass. J Exp Biol 198:805–815.

Krothapalli A, Lourenco L, Shih C. 1997. Visualization of velocity and vorticity fields. In: Nakayama Y, Tanida Y, editors. Atlas of visualization. III. Boca Raton, FL: CRC Press. p 69–82.

Lauder GV. 2000. Function of the caudal fin during locomotion in fishes: kinematics, flow visualization, and evolutionary patterns. Am Zool 40:101–122.

Lauder GV, Jayne BC. 1996. Pectoral fin locomotion in fishes: testing drag-based models using three-dimensional kinematics. Am Zool 36:567–581.

Pridmore PA. 1995. Submerged walking in the epaulette shark *Hemiscyllium ocellatum* (Hemiscylliidae) and its implications for locomotion in rhipidistian fishes and early tetrapods. Zoology 98:278–297.

Raffel M, Willert C, Kompenhans J. 1998. Particle image velocimetry: a practical guide. Heidelberg: Springer-Verlag.

Simons JR. 1970. The direction of the thrust produced by the heterocercal tails of two dissimilar elasmobranchs: the Port Jackson shark, *Heterodontus portusjacksoni* (Meyer), and the piked dogfish, *Squalus megalops* (Macleay). J Exp Biol 52:95–107.

Simons M. 1994. Model aircraft aerodynamics. Herts, UK: Argus Books.

Smith HC. 1992. The illustrated guide to aerodynamics. New York: TAB Books.

Thomson KS. 1976. On the heterocercal tail in sharks. Paleobiology 2:19–38.

Videler JJ. 1993. Fish swimming. New York: Chapman and Hall.

Webb PW. 1989. Station-holding by three species of benthic fishes. J Exp Biol 145:303–320.

Webb PW. 1993. The effect of solid and porous channel walls on steady swimming of steelhead trout *Oncorhynchus mykiss*. J Exp Biol 178:97–108.

Webb PW, Gerstner CL, Minton ST. 1996. Station-holding by the mottled sculpin, *Cottus bairdi* (Teleostei: Cottidae), and other fishes. Copeia 1996:488–496.

Wilga CD, Motta PJ. 1998a. Feeding mechanism of the Atlantic guitarfish *Rhinobatos lentiginosus*: modulation of kinematic and motor activity. J Exp Biol 201:3167–3184.

Wilga CD, Motta PJ. 1998b. Conservation and variation in the feeding mechanism of the spiny dogfish *Squalus acanthias*. J Exp Biol 201:1345–1358.

Wilga CD, Lauder GV. 1999. Locomotion in sturgeon: function of the pectoral fins. J Exp Biol 202:2413–2432.

Wilga CD, Lauder GV. 2000. Three-dimensional kinematics and wake structure of the pectoral fins during locomotion in leopard sharks, *Triakis semifasciata*. J Exp Biol 203:2261–2278.

Wilga CD, Wainwright PC, Motta PJ. 2000. Evolution of jaw depression mechanics in aquatic vertebrates: insights from Chondrichthyes. Biol J Linn Soc 71:165–185.

Zar JH. 1996. Biostatistical analysis, 3rd ed. Upper Saddle River, NJ: Prentice Hall.